Learning remaining useful life with incomplete health information: A case study on battery deterioration assessment

Luciano Sánchez [a,*], Nahuel Costa [a], José Otero [a], David Anseán [b], Inés Couso [c]

[a] *Dpto. Informática, Universidad de Oviedo, Spain*
[b] *Dpto. Ingeniería Eléctrica, Electrónica, C. y S., Universidad de Oviedo, Spain*
[c] *Dpto. Estadística e I.O. y D.M., Universidad de Oviedo, Spain*

ARTICLE INFO

ABSTRACT

This study proposes a method for developing equipment lifespan estimators that combine physical information and numerical data, both of which may be incomplete. Physical information may not have a uniform fit to all experimental data, and health information may only be available at the initial and final periods. To address these issues, a procedure is defined to adjust the model to different subsets of available data, constrained by feasible trajectories in the health status space. Additionally, a new health model for rechargeable lithium batteries is proposed, and a use case is presented to demonstrate its efficacy. The optimistic (max–max) strategy is found to be the most suitable for diagnosing battery lifetime, based on the results.

1. Introduction

Obtaining labelled data for predicting the State of Health (SoH) and Remaining Useful Life (RUL) of a system is challenging because it is not always feasible to measure the system's health using non-destructive procedures. Generally, RUL prediction models are trained using data from systems that have already failed, resulting in training sets that only contain data from deteriorated systems. Consequently, the labels are incomplete, with health information available only at the initial instant (when the system is undamaged) and at the final instant (when it has reached the end of its life). Although partial information is available during the intermediate periods (because health is known to evolve monotonically), conventional supervised learning is not possible. This has led to three groups of approaches to address the issue, as reviewed in [1]: discrete-state and steady-state deterioration models for systems with observable state [2], proportional hazard models (PHM) for dynamic environments [3], and discrete-space methods associated with Markov processes [4].

Steady-state models aim to predict the probability distribution of lifetime based on the system's past state variables, often using stochastic processes such as Brownian motion [5], Gamma processes [6], or Inverse Gaussian [7]. However, the use of steady-state models may be limited by real-world constraints, such as an imperfect fit of the theoretical model or time-varying environments. To overcome these limitations, researchers have studied combining stochastic methods with machine learning techniques using pre-existing run-to-failure data,

and how to make resilient estimates to imperfect inspection data, as discussed in [8,9], and [10].

In this study we propose a procedure for learning RUL from partially unlabelled datasets by introducing constraints based on the system's causes of deterioration. This results in a family of probability distributions of equipment health, sharing properties with certain maximum likelihood inference procedures for incomplete data. In previous research [11], an informed learning algorithm was proposed that incorporates physical knowledge (a set of imprecise differential equations) into a possibility distribution of the system's health state over time. The current work presents a variation of that approach, where imprecision in the physical knowledge is resolved by discarding the inconsistent portion of the training set. A set of models will be defined, each adapted to a family of subsets of the training set. The same max–max, max–min, and min–max-regret strategies presented in [12] will be extended to this problem.

The procedure being developed will be customised to determine the health status of rechargeable lithium-ion batteries, which is crucial for economic and safety reasons. For instance, in medical applications such as pacemakers or implanted defibrillators, anticipating deterioration that could jeopardise the equipment's operation is critical. In transport, preventing degradations that limit electric vehicle autonomy or affect passenger safety is necessary. Additionally, battery failures in consumer electronics can impact equipment performance and result in fires or

accidents [13]. From an economic perspective, repairing batteries for some portable devices can be more expensive than replacing the entire equipment. In other cases, such as electric vehicles, batteries account for a significant portion of equipment costs.

Current research is focused on developing condition-based predictive maintenance procedures that can anticipate battery degradation before failure [14]. Steady-state models, like the one proposed in this study, are effective in estimating the remaining useful life (RUL) of batteries [15]. Specifically, this study builds upon a previous publication [16] that introduced a similar procedure based on empirical risk minimisation.

1.1. Novelty and contribution

This study is an extended version of the Ref. [16], where a specific procedure for battery health diagnosis was defined. This version provides a theoretical basis to extend this procedure to a broader category of problems, keeping the application to batteries as an example of application. In particular, the novelties of this paper with respect to the previous version are:

- A methodology for learning health models from both data and physical information about the system, which effectively handles uncertainty in both types of information.
- The implementation of max–max, max–min, and min–max-regret criteria for selecting a consistent subset of training data in lifetime estimation problems.
- A new health model definition for lithium-ion batteries with a negative electrode consisting of graphite and silicon.

1.2. Overview

The structure of this paper is as follows: Section 2 introduces the theoretical problem, defines the health model and particularises the strategies for choosing parameters in the face of incomplete information. In Section 3 the problem is particularised to the study of battery deterioration. A simplified electrochemical model is proposed and the alternatives introduced in the previous section are implemented. Section 4 develops an empirical study with real and simulated batteries. The conclusions of the study are presented in Section 5. Appendix includes additional details on the degradation mechanisms of batteries of the type used in the empirical study.

2. RUL learning from positive and weakly labelled examples

This section proposes a method for estimating the lifetime of a system from a physical model and from measured data on a system that has developed a failure. The physical model consists of a set of differential equations and depends on hidden variables that can only be known indirectly.

2.1. Notation

Let $\mathbf{u}_t$ be the vector of inputs to the system at time t, $\mathbf{y}_t$ the vector of outputs and $\mathbf{x}_t$ the vector of hidden (not directly observable) state variables. The physical model of the system consists of a pair of time-varying, non-linear differential equations defined by two functions $f(\cdot)$ and $g(\cdot)$, belonging to a given parametric family:

$$\dot{\mathbf{x}}_t = f(\mathbf{x}_t, \mathbf{u}_t, \theta_t) \tag{1}$$

$$\hat{\mathbf{y}}_t = g(\mathbf{x}_t, \mathbf{u}_t, \theta_t) \tag{2}$$

A training set is available, which is a sequence of the observable inputs and outputs $\mathbf{D} = [\mathbf{u}_t, \mathbf{y}_t]_{t=1}^T$ of the system at a set of time instants $t = 1, \ldots, T$. The true SoH of the system cannot be observed but in the

first ($t = 1$) and last ($t = T$) time periods. The SoH model is a function of the same parameter θ_t:

$$\widehat{\mathrm{SoH}}(\theta_t) \in [0, 1] \tag{3}$$

The SoH takes the value 1 when the system has no deterioration and 0 when it has reached its end of life. In this study it is understood that the SoH is the quotient between the life expectancy at instant t and the expected life at $t = 1$, thus

$$\mathrm{RUL}(t) = \mathrm{RUL}(1) \cdot \mathrm{SoH}(\theta_t). \tag{4}$$

We will use the notation $\theta = (\theta_1, \ldots, \theta_T)$ to refer to the set of parameters that define f and g over time. It will be considered that by "model learning" we mean estimating, according to criteria to be discussed later, a parameter $\hat{\theta}$ from the training set $\mathbf{D}$. Finally, by "learning algorithm" we mean a function $\mathcal{L}$ that produces an estimate $\hat{\theta}$ from $\mathbf{D}$:

$$\hat{\theta} = \mathcal{L}(\mathbf{D}) \tag{5}$$

2.2. Dealing with uncertainty in data and model

In general, the $\hat{\mathbf{y}}_t$ predictions of the model will not correspond exactly to the $\mathbf{y}_t$ measurements of the training set for a number of reasons. On the one hand, it will be assumed that there are inputs to the system that are not being modelled. The influence of these unmodelled inputs on the output will be treated as random noise. On the other hand, a second type of uncertainty, of an epistemic nature, will also be considered. This uncertainty arises when the available physical information about the system (the Eqs. (1) and (2) mentioned above) is approximate and therefore a perfect fit of the model parameters to all training data is not possible, even if these data were not contaminated with noise.

In fully data-driven (or "black box") models, a differentiated treatment of epistemic uncertainty is usually not necessary, as it can be reduced by increasing the complexity of the model. However, when physical knowledge and data are integrated, it cannot be ruled out that the a priori knowledge is inaccurate, so that a non-stochastic uncertainty is being introduced into the problem. In this study, as in other work on Physically Informed Learning (PIL) [17], physical knowledge will be incorporated by introducing constraints on the objective function of the learning problem in order to reduce the solution space [18]. If an incorrect constraint were introduced, it would be possible for the solution of the problem to fall outside the feasible area; this is a problem that has only recently begun to be studied [19].

In particular, as will be seen in the next sections, we will assume that the degradation of the system is defined by a matrix with the deterioration rate of each component of the system at each instant of time. Each element of this matrix depends on the same vector of parameters θ_t as the equations that define the physical knowledge about the problem (see Eqs. (1), (2) and (3)). These equations are simplifications of reality and therefore a perfect fit to the data cannot be expected; alternatively, parameter values may be found for which the model correctly explains one part of the data and does not fit others. Reciprocally, if we list all the subsets of the data that can be explained by some parameter value, we end up with a set of parameters, which contains all those values that explain at least part of the training set. This set-valued estimate of θ_t will, in turn, give rise to a set-valued estimate of the health of the system at each instant in time. This treatment has precedents in some methods used to select consistent subsets of data in inverse problems [20]. The aim is to identify the minimum area region in the parameter space that explains the entire training data set. Finally, as mentioned above, we will employ procedures similar to those developed for maximum likelihood estimation from imprecise data [12] to estimate the health of the system and its remaining lifetime.

2.3. State of health model

We will call P_y the joint probability of the output of the system and the model. The empirical likelihood function is denoted as

$$\ell_1(\theta, \mathbf{D}) = \prod_{t=1}^{T} P_y(\hat{y}_t, y_t \mid \theta) \tag{6}$$

and we will denote $\mathcal{L}_1$ the learning algorithm that returns the value of the parameter that maximises this empirical likelihood

$$\ell_1(\mathcal{L}_1(\mathbf{D}), \mathbf{D}) = \arg\max_{\theta} \ell_1(\theta, \mathbf{D}). \tag{7}$$

As in Ref. [11], we will assume that the system is subject to different types of deterioration at the same time. We will denote C the set of deterioration types and call $\mathrm{SoH}^c(\theta_t)$ the health of the system relative to the deterioration of type $c \in C$. The relative healths are related to the health of the whole system as follows:

$$\widehat{\mathrm{SoH}}(\theta_t) = \min_{c \in C} \widehat{\mathrm{SoH}}^c(\theta_t). \tag{8}$$

On the other hand, the SoH will also be considered to be maintained or decreased over time. The $\mathcal{L}_1$ algorithm does not guarantee this condition, so several restrictions must be added to it.

On the one hand, the periods between the first and the penultimate are not labelled. Our knowledge is limited to

$$\mathrm{SoH}(\theta_1) = 1 \tag{9}$$

$$\mathrm{SoH}(\theta_T) = 0 \tag{10}$$

$$\mathrm{SoH}(\theta_t) \le \mathrm{SoH}(\theta_{t-1}) \tag{11}$$

For this reason, we can define a rate of deterioration $\delta_t^c \in [0, 1]$ as

$$\delta_t^c = \frac{\widehat{\mathrm{SoH}}^c(\theta_t)}{\widehat{\mathrm{SoH}}^c(\theta_{t-1})} \tag{12}$$

and establish that the feasible region Γ of the parameter set is composed of the values of θ that can be expressed by means of any suitable matrix $[\delta_t^c]$, with T rows and $\#C$ columns, where

$$\begin{aligned}
\theta \in \Gamma \iff & \exists [\delta_t^c] \in [0,1]^{(\#C \times T)} \\
& \text{with} \delta_c^1 = 1 \; \forall c \in C, \\
& \quad \min_{c \in C} \delta_c^T = 0, \\
& \quad \min_{c \in C} \delta_c^T > 0 \, \text{for} \, t = 2, \dots, T-1, \\
& \text{s.t.} \widehat{\mathrm{SoH}}(\theta_t) = \min_{c \in C} \prod_{\tau=1}^{t} \delta_\tau^c \quad \forall t = 1, \dots, T
\end{aligned} \tag{13}$$

On the other hand, each matrix $[\delta_t^c]$ can be associated with a subset of the feasible space $\Theta([\delta_t^c]) \subset \Gamma$, whose associated models have an evolution in SoH compatible with that deterioration matrix:

$$\Theta([\delta_t^c]) = \{\theta \in \Gamma : \widehat{\mathrm{SoH}}(\theta_t) = \min_{c \in C} \prod_{\tau=1}^{t} \delta_\tau^c, \quad \text{for} \, t = 1, \dots, T\} \tag{14}$$

so that the likelihood of this deterioration rate matrix can be defined as

$$\ell_2([\delta_t^c], \mathbf{D}) = \begin{cases} \sup\{\ell_1(\theta, \mathbf{D}) : \theta \in \Theta([\delta_t^c])\} & \text{if } \Theta([\delta_t^c]) \ne \emptyset \\ 0 & \text{else} \end{cases} \tag{15}$$

Lastly, we will denote $\mathcal{M}$ the mapping

$$[\hat{\delta}_t^c] = \mathcal{M}(\mathbf{D}) \tag{16}$$

that returns the deterioration matrix that maximises the empirical likelihood of the deterioration rate

$$\ell_2(\mathcal{M}(\mathbf{D}), \mathbf{D}) = \max_{M} \ell_1(M, \mathbf{D}) \text{with} M \in [0,1]^{(\#C \times T)}. \tag{17}$$

and a learning algorithm $\mathcal{L}_2$ that returns the parameter of the most likely model whose SoH is feasible

$$\ell_1(\mathcal{L}_2(\mathbf{D}), \mathbf{D}) = \max_{\theta \in \Theta(\mathcal{M}(\mathbf{D}))} \ell_1(\theta, \mathbf{D}) \tag{18}$$

2.4. Implementation of max–max, min–max and min–max-regret strategies

In different practical cases (including the problem related to battery deterioration discussed below) models based on differential equations are a simplification of reality. This means that the model will not have a homogeneous fit at all points in the sample. This is a common problem in supervised learning (think, for example, of the treatment of outliers in regression problems) but in this context it is not immediately obvious which parts of the dataset $\mathbf{D}$ should be discarded so that the maximum likelihood estimate of the model deterioration rates is the model that most closely describes the actual evolution of the health state. Moreover, as will be seen below, there are practical problems where the subset of $\mathbf{D}$ to be discarded depends on the deterioration mode, so it is not possible to perform instance selection and discard inconsistent values before model fitting.

Let us suppose that the indices of the most informative elements in $\mathbf{D}$ belong to an unknown set $\mathbf{S} \subset \{1, \dots, T\}$, and let $\mathbf{S}_t = \mathbf{S} \cap \{1, \dots, t\}$. First, we define the incremental datasets

$$\mathbf{D}_t(\mathbf{S}) = [\mathbf{u}_\tau, \mathbf{y}_\tau]_{\tau \in \mathbf{S}_t} \tag{19}$$

with the values of the observed variables in the system at the instants in $\mathbf{S}_t$. Let $M_t(\mathbf{S})$ be a submatrix of the deterioration rates, $M_t = [\delta_\tau^c]$ with $\tau \in \mathbf{S}_t$, $c \in C$. The sequence of likelihoods of the models obtained by applying the $\mathcal{L}_2$ algorithm to the successive sets $\mathbf{D}_t$ are

$$L([\delta_t^c], \mathbf{S}) = [\ell_2(M_1(\mathbf{S}), \mathbf{D}_1(\mathbf{S})), \dots, \ell_2(M_T(\mathbf{S}), \mathbf{D}_T(\mathbf{S}))] \tag{20}$$

If the set $\mathbf{S}$ is not known, but a family $\mathbb{S} \supset \mathbf{S}$ of alternatives is available, a sequence of sets of likelihood values will be available

$$L([\delta_t^c], \mathbb{S}) = [\ell_2(M_t(\mathbf{S}), \mathbf{D}_t(\mathbf{S})) : \mathbf{S} \in \mathbb{S}]_{t=1}^{T} \tag{21}$$

and the value of the parameter $[\delta_t^c]$ can be chosen with different strategies. In the specialised literature, the following three options have been studied the most:

1. max–max strategy: This consists of choosing the parameter that maximises the product of the likelihoods at each time instant. In the case where $\{1, \dots, T\} \in \mathbb{S}$, this strategy coincides with the $\mathcal{L}_2$ algorithm.
2. Min–max strategy: This consists of choosing the best parameter in the worst case. In this context, to each deterioration matrix $[\delta_t^c]$, the smallest component of $L([\delta_t^c], \mathbb{S})$ would be assigned, and the deterioration matrix that maximises that value would be sought.
3. Min–max-regret strategy: The regret of choosing a deterioration different from the most likely one is minimised at each time instant. The regret value of choosing a set of indices $\mathbf{R}$ at time t is

$$\mathrm{regret}(\mathbf{R}, t) = \frac{\ell_2(M_t(\mathbf{R}), \mathbf{D}_t(\mathbf{R}))}{\max_{\mathbf{S} \in \mathbb{S}} \ell_2(M_t(\mathbf{S}), \mathbf{D}_t(\mathbf{S}))} \tag{22}$$

Each deterioration matrix is assigned the maximum regret value, and the matrix that minimises this maximum is chosen.

3. Particularisation to battery deterioration

The method defined in the previous section is particularised for the estimation of the SoH of rechargeable lithium-ion batteries in this section. In order to define the knowledge-based criteria for determining whether or not the battery health is compatible with the history of the system variables, a brief description of the battery parts that are subject to deterioration, and to the latent and observable variables of this type of systems, is first provided.

3.1. Electrochemical battery model

The battery terminal voltage is the difference between the positive and negative electrode potentials. Each electrode has a resting potential that depends on its degree of lithiation, which is the ratio of the number of moles of lithium ion intercalated in the active material to its capacity. The electrode potential increases when current flows through it [21], non-linearly with the value of the current.

In this study we will analyse a recent type of high-capacity batteries in which the negative electrode is composed of a mixture of materials: graphite and silicon [22]. We will refer to the moles of lithium ion at the positive electrode as l_{PE}, to the capacity of the positive electrode as c_{PE} and to the potential of the positive electrode as V_{PE}. Similarly, at the negative electrodes of graphite and silicon the moles of lithium ion are called l_{Gr} and l_{Si}, the potentials are called V_{Gr} and V_{Si} and the capacities are c_{Gr} and c_{Si}.

When a positive electric current $I(t)$ (discharge current) flows through the battery, lithium ions are displaced from the positive to the negative electrode, and when the current is negative, lithium ions are displaced from the negative to the positive electrode. For low currents, it can be assumed without excessive error that the electrodes are in equilibrium at any instant of time. This equilibrium is described by the following equations:

$$V_{Gr}(l_{Gr}(t)/c_{Gr}(t), I_{Gr}(t)) = V_{Si}(l_{Si}(t)/c_{Si}(t), I_{Si}(t))$$
$$I_{Gr}(t) + I_{Si}(t) = I(t)$$
(23)

The voltage at the battery terminals is

$$V_{BAT}(t) = V_{PE}(l_{PE}(t)/c_{PE}(t), I(t)) - V_{Gr}(l_{Gr}(t)/c_{Gr}(t), I_{Gr}(t)).$$
(24)

For low currents, assuming that all electrochemical processes are in equilibrium, the terminal voltage of the battery therefore depends on the following:

- The initial lithiation states of electrodes
- The capacities of each electrode
- The battery charge
- The charging or discharging current

This dependency is expressed as follows:

$$V_{BAT}(t) = V_{PE}((l_{PE}(0) - Q(t))/c_{PE}(t), I(t)) -$$
$$V_{Gr}((l_{Gr}(0) + Q(t))/c_{Gr}(t), I_{Gr}(t))$$
(25)

where

$$I(\tau) = \left.\frac{dQ}{dt}\right|_{\tau}$$
(26)

$$I(t) = I_{Gr}(t) + I_{Si}(t)$$
(27)

$$Q(t) = Q_{Gr}(t) + Q_{Si}(t) - Q_{Gr}(0) - Q_{Si}(0)$$
(28)

$$V_{Gr}((l_{Gr}(0) + Q_{Gr}(t))/c_{Gr}(t), I_{Gr}(t)) =$$
$$V_{Si}((l_{Si}(0) + Q_{Si}(t))/c_{Si}(t), I_{Si}(t))$$
(29)

Using the notation of the previous section, the input variable is the current, the output is the battery terminal voltage and the state variables are the amount of lithium in each electrode and their capacities:

$$\mathbf{x}(t) = (l_{Gr}, l_{Si}, l_{PE}, c_{Gr}, c_{Si}, c_{PE})$$
(30)

$$\mathbf{y}(t) = V_{BAT}$$
(31)

$$\mathbf{u}(t) = I(t)$$
(32)

3.2. Observable and latent variables

During battery use, certain phenomena occur that reduce the capacities of the electrodes or the mobility of the lithium. These degradation processes reduce the battery's capacity to store an electrical charge, and thus the battery's service life.

For the purposes of this study, the SoH of a battery depends on five latent (i.e. not directly observable) variables. Assuming the battery is discharged at time t_0, the values of these variables at time $t \geq t_0$ are:

1. z_1: The capacity of the positive electrode, $c_{PE}(t)$.
2. z_2: The capacity of the graphite in the negative electrode, $c_{Gr}(t)$.
3. z_3: The capacity of the silicon in the negative electrode, $c_{Si}(t)$.
4. z_4: The amount of lithium in the positive electrode when the battery was discharged, $l_{PE}(t_0)$.
5. z_5: The amount of lithium in the negative electrode when the battery was discharged, $l_{Gr}(t_0) + l_{Si}(t_0)$.

The charge capacity CAP of the battery is limited by the amount of lithium in the negative electrode that can be transported to the positive electrode (the "lithium inventory") but also by the free space in the positive electrode that receives it (both measured when the battery was discharged, at time t_0). The capacities of the electrodes can also shrink in time, thus at time t

$$CAP(t) = \min(l_{Gr}(t_0) + l_{Si}(t_0), c_{PE}(t) - l_{PE}(t_0), c_{Gr}(t) + c_{Si}(t))$$
(33)

$$= \min(z_5(t_0), z_1(t) - z_4(t_0), z_2(t) + z_3(t_0))$$
(34)

Let the vector of latent variables at time t be

$$\mathbf{z}(t) = (z_1(t), \dots, z_5(t))$$
(35)

and let

$$\mathbf{Z}(t) = [\mathbf{z}(t_0), \dots, \mathbf{z}(t)]$$
(36)

be the matrix containing the history of the values of the latent variables since $t = t_0$, when the battery was discharged. We define three deterioration modes:

$$SoH^1(\mathbf{Z}) = z_5(t)/CAP(0)$$
(37)

$$SoH^2(\mathbf{Z}) = (z_1(t) - z_4(t_0))/CAP(0)$$
(38)

$$SoH^3(\mathbf{Z}) = (z_2(t) + z_3(t))/CAP(0)$$
(39)

and the SoH of the battery is

$$SoH(\mathbf{Z}) = \min(SoH^1(\mathbf{Z}), SoH^2(\mathbf{Z}), SoH^3(\mathbf{Z}))$$
(40)

Finally, we would like to point out that not all deterioration modes affect battery capacity instantaneously. Health is the minimum of three values (recall Eq. (8)), and the evolution of one of the modes may not reduce the capacity until it becomes the main deterioration mode. The RUL estimator takes these hidden evolutions into account, as extrapolation of charge capacity over time can have abrupt changes in slope when one of the non-visible modes becomes the predominant mode. A high proportion of works applying machine learning to predict health evolution do not take into account this [23], so incorporating physical knowledge into learning allows for better results than merely modelling the evolution of observable variables.

3.3. Implementation of maximum likelihood strategies

Fig. 1 shows the battery terminal voltage, positive and negative electrode voltages and model predictions during a low-current charge/discharge cycle of a rechargeable lithium-ion battery. Fig. 2 shows the evolution of these curves during normal battery ageing. Please note that the electrode potentials, namely V_{PE}, V_{Gr}, and V_{Si}, depend on the sign of the charging current. However, we have excluded this hysteresis effect from the model discussed in the previous section to keep the explanation simple.

It is worth noting that the potential curve of the positive electrode experiences an abrupt variation when the battery is completely discharged. However, this variation does not affect the voltage observed at the battery terminals in most cases, except when the positive electrode is severely degraded. On the other hand, the negative electrode's potential curve also exhibits a similar abrupt variation, but this variation can significantly impact the battery voltage. Therefore, at states of charge lower than 5%, even a slight inaccuracy in determining the internal state can result in a significant change in the model's prediction. To
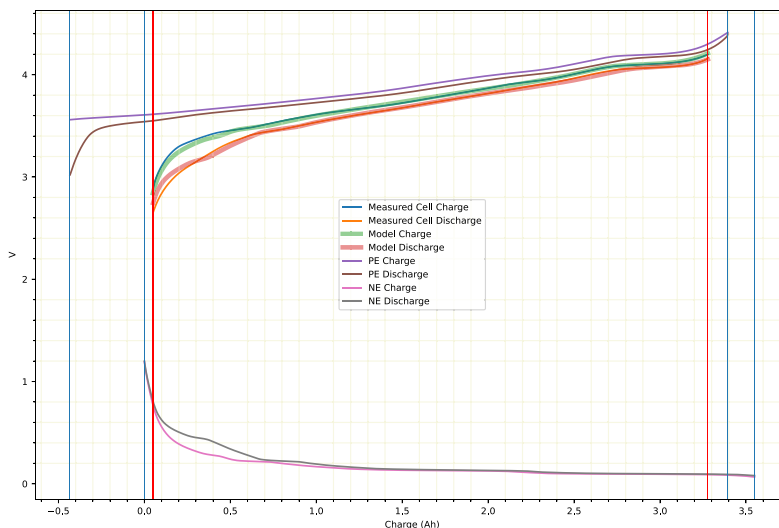
Fig. 1. Battery terminal voltages, positive and negative electrode voltages and model predictions during a low current charge and discharge cycle.
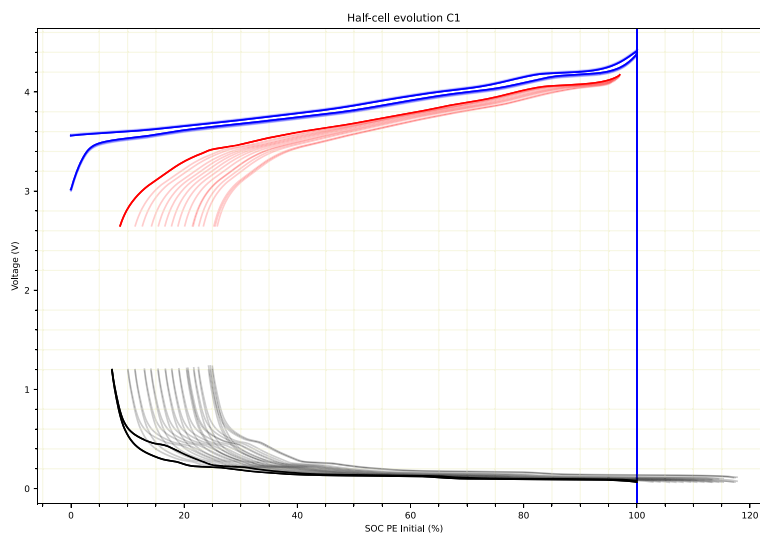

Fig. 2. Evolution of the battery terminal voltage, positive and negative electrode voltages during normal ageing of the battery.

avoid this issue, it is common practice in the specialised literature to disregard periods of the training set where the charge is very low [15].

The same reasoning can be applied to very high states of charge (greater than 95%). On the other hand, not all battery deteriorations (as detailed in the Appendix) can be detected in the same way during both the charge and discharge half cycles. In case the model is trained using only one charge cycle or one discharge cycle, the diagnosis of the battery's health will differ from when the model is trained on the entire battery dataset. This difference can be observed clearly in the incremental capacity curves (ICA curves [24]), which are commonly used for health diagnostic tasks and represent the charge derivative versus voltage curve [25] (see Fig. 3).

4. Empirical study

To facilitate benchmarking of results by battery experts, in addition to making RUL and health predictions, the mechanisms of battery deterioration will be analysed by means of some metrics commonly used in the literature [26]. These metrics are described in the Appendix for the convenience of the reader.

Experiments are divided into three parts. In the first part, the proposed algorithm is applied to Li-Ion batteries simulated using the ALAWA tool [27]. The reason for using simulated batteries is to validate the deterioration learning algorithm in problems with known outcome, to assess the degree of fit of the proposed alternative and to compare it with other uninformed learning techniques. In the second and third parts, the method is applied to real batteries. First, the deterioration of a battery is analysed numerically, showing the difference between different types of diagnosis. Finally, the deterioration diagnosis of four cells, two of them with normal ageing and two with accelerated ageing, is shown, showing the influence of the subset of the training dataset on the diagnostic conclusions.

4.1. Simulated batteries

A realistic synthetic 5 Ah battery has been simulated. The positive electrode is NMC (Nickel, Manganese and Cobalt) and the negative electrode consists of a combination of graphite and silicon [28]. The capacity of the positive electrode is 5.55 Ah. The capacities of the graphite and silicon in the negative electrode are 4.5 Ah and 0.5 Ah, respectively. The positive electrode is 90% lithiated at the beginning of the charge and is completely de-lithiated at the end of the charge. The negative electrode of the non-deteriorated battery is fully delithiated at
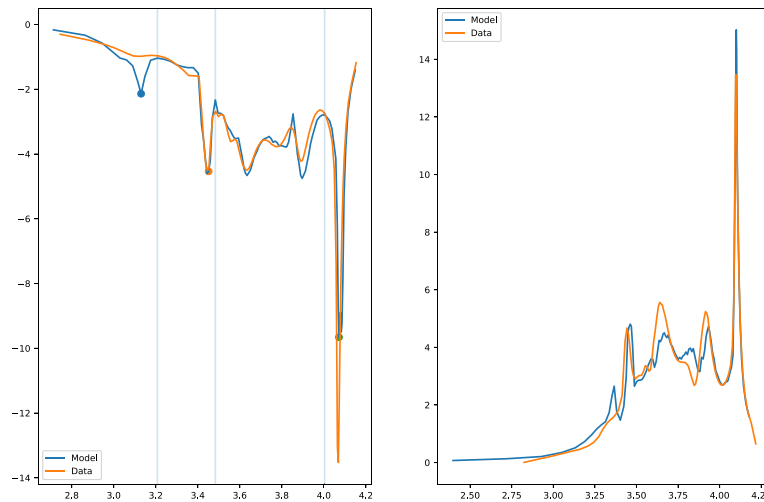
Fig. 3. Incremental capacity curves at discharge (left) and charge (right) showing that the derivative of the charge with respect to the voltage is different in the charge and discharge half-cycles.

Table 1
Comparative results of uninformed and physical-informed learning for the seven defect types.

Deterioration	$\mathcal{L}_1$	Informed learning			
		$\mathcal{L}_2(\mathbf{D})$	$\mathcal{L}_2(\mathbb{S})$-MM	$\mathcal{L}_2(\mathbb{S})$-Mm	$\mathcal{L}_2(\mathbb{S})$-mMR
LLI	0.63	0.42	**0.40**	0.71	0.64
LAMdPE	3.81	2.25	**0.55**	3.28	3.07
LAMdGr	0.99	**0.55**	1.98	1.24	1.23
LAMdSi	1.37	0.66	**0.54**	1.61	1.78
LAMlPE	1.07	0.88	0.88	**0.76**	0.80
LAMlGr	0.81	0.58	0.53	**0.25**	0.25
LAMlSi	1.43	0.88	**0.79**	1.48	1.24
Average	1.45	0.89	**0.81**	1.33	1.29
Average PE	2.44	1.56	**0.72**	2.02	1.93
Average NE	1.15	**0.67**	0.96	1.15	1.13

Table 2
Comparative results of uninformed and informed learning for the seven defect types. All optimisations include a L_1 regularisation term.

Deterioration	$\mathcal{L}_1$	Regularised informed learning			
		$\mathcal{L}_2(\mathbf{D})$	$\mathcal{L}_2(\mathbb{S})$-MM	$\mathcal{L}_2(\mathbb{S})$-Mm	$\mathcal{L}_2(\mathbb{S})$-mMR
LLI	0.63	0.05	**0.02**	0.08	0.06
LAMdPE	3.81	1.64	**0.55**	3.30	2.69
LAMdGr	0.99	0.10	**0.01**	0.71	0.54
LAMdSi	1.37	0.30	**0.22**	1.36	1.33
LAMlPE	1.07	0.18	0.27	0.19	**0.14**
LAMlGr	0.81	0.58	0.39	**0.24**	0.26
LAMlSi	1.43	**0.41**	0.42	1.45	0.46
Average	1.45	0.47	**0.28**	1.05	0.78
Average PE	2.44	0.91	**0.41**	1.74	1.42
Average NE	1.15	0.35	**0.28**	0.93	0.65

the beginning of the charge and fully lithiated at the end of the charge. The initial values of the parameter vector are therefore

$$\theta^0 = \left(\frac{5}{0.9}, 4.5, 0.5, 5, 0 \right)$$

Starting from the same initial conditions, seven simulations of 2000 cycles were carried out, each with a single type of deterioration. The average of the percentage errors of the electrode capacities and lithium inventory was used as a metric for the model fit.

The family of subsets used in this part of the experimentation has the following elements: $\mathbb{S} = \{\mathbf{S}_1, \mathbf{S}_2, \mathbf{S}_3\}$:

$$\mathbf{S}_1 = \{t : I(t) > 0, Q(t) \geq 0.05 \cdot \text{CAP}(t), Q(t) \leq 0.95 \cdot \text{CAP}(t)\} \quad (41)$$

$$\mathbf{S}_2 = \{t : I(t) < 0, Q(t) \geq 0.05 \cdot \text{CAP}(t), Q(t) \leq 0.95 \cdot \text{CAP}(t)\} \quad (42)$$

$$\mathbf{S}_3 = \{t : Q(t) \geq 0.05 \cdot \text{CAP}(t), Q(t) \leq 0.95 \cdot \text{CAP}(t)\} \quad (43)$$

Table 1 shows the errors obtained by the unconstrained algorithms (learning algorithm $\mathcal{L}_1$) and those of the models proposed in this study. The $\mathcal{L}_2(\mathbf{D})$ column contains the results of the empirical likelihood minimisation over the full charge and discharge cycle. The $\mathcal{L}_2(\mathbb{S})$-MM column is the max–max strategy. The $\mathcal{L}_2(\mathbb{S})$-Mm column is the maximin strategy. The $\mathcal{L}_2(\mathbb{S})$-mMR column is the min–max-regret strategy.

The mean error is better in models with informed learning, the version that offers the best results is the minimin/optimistic alternative. This is an expected result, as the optimistic version is robust to coarsening processes [29]. The pessimistic or minimin-regret versions try to minimise the wrong risk in those phases of the cycle where deteriorations do not manifest themselves.

4.1.1. Regularised learning

The experiments have been repeated by adding a regularisation term to all optimisation problems where the modulus of the matrix $[\delta_t^c]$ is penalised. Table 2 shows the errors of the regularised versions, which support the same conclusions drawn from Table 1. In this case, the use of regularisation of type L_1, which leads to a sparse deterioration vector, improves the results because each battery has undergone a single deterioration process in the validation data (i.e., the optimal solution of each problem is a vector in which all components are zero except one; the regularisation penalises solutions with more than one concurrent deterioration and is therefore expected to improve the results of this method for this particular validation set.)

4.2. Actual batteries (I)

The results obtained in synthetic batteries show that the informed strategy, in its optimistic version, has the best accuracy in estimating the type and intensity of deteriorations. It has also been shown that the addition of a regularisation term is beneficial, provided that the assumption that the number of concurrent deterioration types is low is accepted.

In simulated batteries the model prediction error is close to zero. It is worth asking whether the model approximation error in a real battery will cancel out the differences between the techniques studied or whether, on the contrary, the improvement in the accuracy of the weak supervision estimation will be relevant in real problems. To study this case we have used a Samsung-SDI INR18650-35E cell, with a standard discharge capacity of 3350 mAh, which was subjected
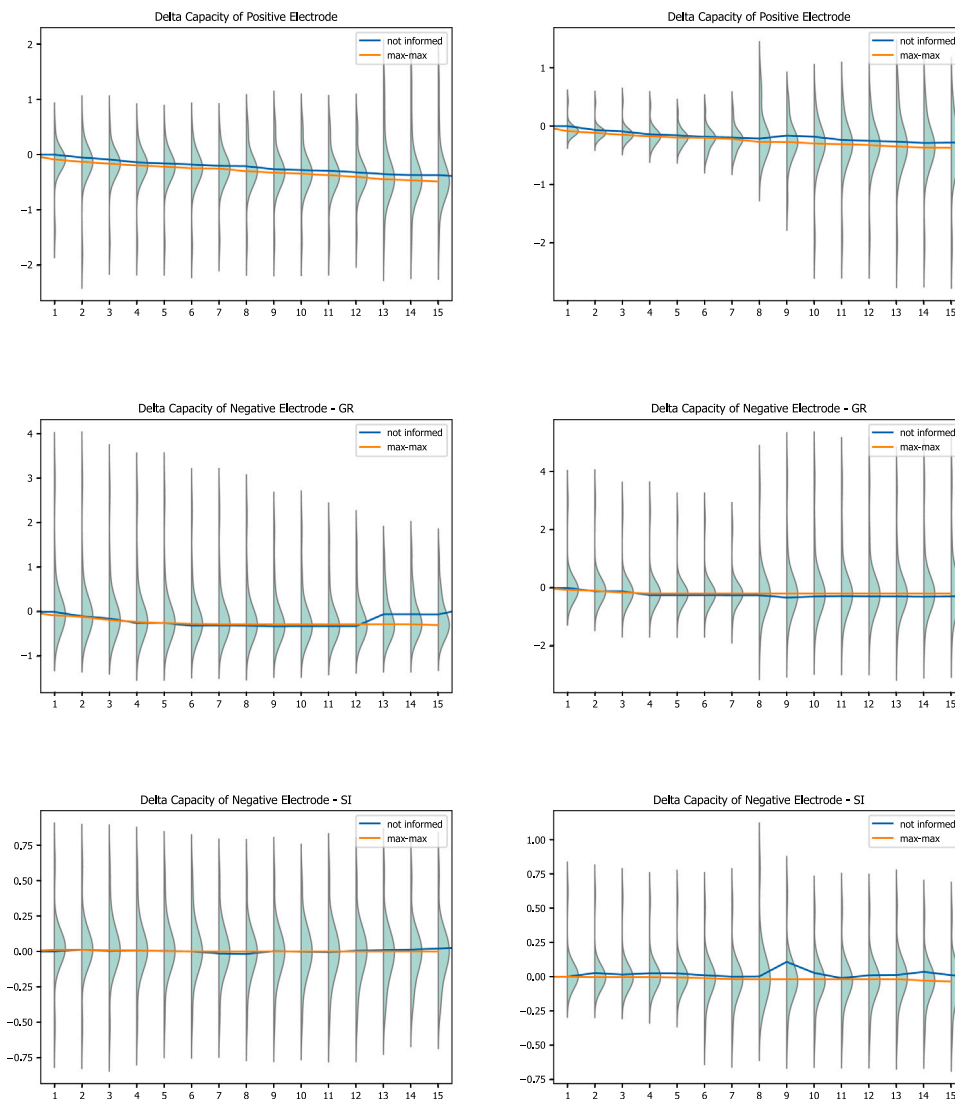
Fig. 4. Cells with normal deterioration. x-axis: cycles (per 100). y-axis: relative increase or loss of capacity with respect to the initial capacity. Left side, from top to bottom: deterioration of the positive electrode, the graphite part of the negative electrode and the silicon part of the negative electrode in cell C1. Right side: the same deterioration in cell C2.

to a standard set of tests [28]. A multichannel, high-precision series Arbin LBT was used to perform the tests and record the voltage and current values. The cell was placed at constant 23 °C in a Memmert environmental chamber.

The deterioration predictions produced by the minimum risk models on the full dataset and with the $\mathcal{L}_2(\mathbb{S})$-MM learning algorithm are shown in Table 3. In this table, we have grouped the LAM degradation modes into three categories: LAMPE (loss of capacitance of the positive electrode), LAMGr (loss of capacitance of the graphite component of the negative electrode), and LAMSi (loss of capacitance of the silicon component of the negative electrode). The differences between the lithium inventory estimates are low ($\approx 1\%$) and the same can be said for the differences in the positive electrode capacity, but the active graphite estimates are much different. The estimate with weak supervision detects deterioration of constant magnitude over the entire battery life, whereas the ordinary estimate indicates that no active graphite is lost from cycle 700 onwards, showing that weakly supervised learning techniques can alter the diagnosis that would be obtained by supervised learning in real problems.

4.3. Actual batteries (II)

Figs. 4 and 5 illustrate the application of the ageing model to four Samsung-SDI INR18650-35E batteries, which are similar to those used in the previous experiment. Specifically, cells C1 and C2 (Fig. 4) underwent normal deterioration over 1700 cycles, while cells C4 and C5 (Fig. 5) reached their end of life after 400 cycles due to a problem in the temperature controlled chamber.

Both figures display similar battery deterioration patterns to demonstrate the variability of the model fits to the data. In the upper left part of Fig. 4, the positive electrode capacity gradually decreases, and the proposed model fit (min-min strategy) does not alter the uninformed model prediction. On the right-hand side, the uninformed algorithm converges to solutions starting at cycle 800, where the electrode capacity increases, which is physically impossible. The proposed algorithm corrects this error. The same circumstance occurs in the evolution of the graphite capacity in cell C1 (left column, middle row) and the silicon capacity in cell C2 (right column, bottom row). The densities shown in the figures represent the conditional probabilities of the model response with respect to reality and are represented by a kernel estimation of the model output density for each of the cycles for the analysed family
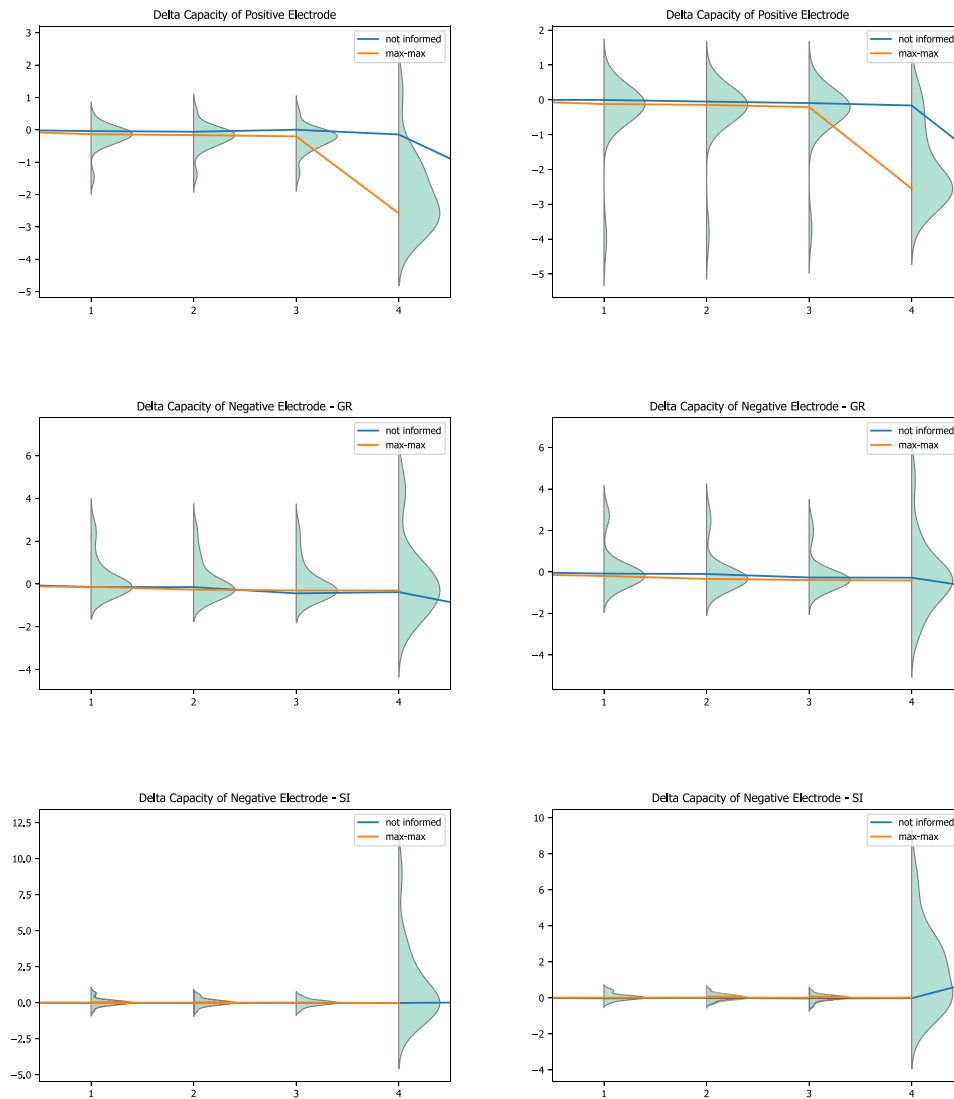
Fig. 5. Cells with abnormal deterioration. x-axis: cycles (per 100). y-axis: relative increase or loss of capacity with respect to the initial capacity. Left side, from top to bottom: deterioration of the positive electrode, the graphite part of the negative electrode and the silicon part of the negative electrode in cell C4. Right side: the same deterioration in cell C5.

Table 3
Deterioration predictions on a real battery. INR18650-35E cell from Samsung-SDI, with standard discharge capacity of 3350 mAh.

Cycle	$\mathcal{L}_2(\mathbf{D})$				$\mathcal{L}_2(\mathbb{S})$-MM			
	LLI	LAMPE	LAMGr	LAMSi	LLI	LAMPE	LAMGr	LAMSi
100	0.00	0.00	0.00	0.00	0.00	0.00	0.00	0.00
200	0.00	0.00	0.00	0.00	0.00	0.00	0.00	0.00
300	3.11	1.79	3.09	0.00	1.64	1.03	0.00	0.00
400	4.36	2.27	3.09	0.00	2.92	1.07	4.71	0.00
500	6.09	3.69	6.45	0.00	4.84	1.84	4.72	0.00
600	7.33	4.21	6.45	0.00	6.11	2.33	4.73	0.00
700	8.52	4.92	7.88	0.00	7.34	2.46	7.59	0.00
800	10.07	5.46	7.88	0.00	9.22	3.63	7.66	0.00
900	10.81	5.76	7.88	0.00	9.76	3.69	7.86	0.00
1000	12.25	6.99	7.88	0.00	11.44	4.83	8.22	0.00
1100	13.23	7.50	7.88	0.00	12.71	6.17	12.01	0.00
1200	13.97	7.87	7.88	0.00	13.37	6.69	12.03	0.00
1300	14.79	8.43	7.88	0.00	14.49	7.28	12.03	0.00
1400	15.82	9.41	7.88	0.00	15.60	7.73	12.03	0.00
1500	16.95	9.89	7.88	0.00	17.84	10.40	12.03	0.00
1600	17.69	10.51	7.88	0.00	17.84	10.60	12.16	0.00
1700	17.69	10.51	7.88	0.00	17.84	10.60	12.16	0.00

of subsets of the training set. In this set of experiments, the family $\mathbb{S}$ consists of charge-only, discharge-only, and combined data, limiting the battery terminal voltage values to lower ranges between 2.8 and 3 V and upper ranges between 3.5 and 4.2 V.

Fig. 5 presents the same analysis for cells C4 and C5, demonstrating that the correction of the reported algorithm in the positive electrode capacity is significantly higher.

5. Concluding remarks and future work

The literature on the use of machine learning for non-destructive diagnosis of battery conditions is extensive, with numerous published algorithms that extract information from current, voltage, and temperature measurements made under different assumptions. This paper proposes a new model for the health status of a battery that relies on both data and physical knowledge. The novelty of this approach is that both types of information are assumed to be imprecise, and the model cannot be uniformly fitted to all available data. Fitting the model to different subsets of the training set produces varying results. Various methods implicitly select instances and use only discharge data, while others select voltage and current values within a specific range of states of charge, disregarding model errors when the battery

is almost charged or discharged. Nonetheless, we claim that the most appropriate subset must be chosen depending on the parameter to be estimated, making it a crucial part of the learning algorithm. Three different types of solutions have been proposed, which return subsets where the fit is maximal (optimistic criterion) or where the fit is best at the worst time instant (pessimistic criteria), and it has been found that in health diagnosis problems, the optimistic criterion is preferable since the subset where the fit is best also includes the best information about the defect.

In future work, we will investigate the extension of the reported procedure to ohmic and faradaic deteriorations. We will validate our results with simulations that include several concurrent faults and study regularisation techniques other than the L_1 criterion analysed in this contribution.

CRediT authorship contribution statement

Luciano Sánchez: Conceptualization, Writing – original draft, Software, Supervision. **Nahuel Costa:** Investigation, Data curation, Reviewing and editing. **José Otero:** Investigation, Reviewing and editing. **David Anseán:** Data curation, Reviewing and editing. **Inés Couso:** Conceptualization, Writing – review & editing, Supervision.

Declaration of competing interest

The authors declare that they have no known competing financial interests or personal relationships that could have appeared to influence the work reported in this paper.

Data availability

Data will be made available on request.

Acknowledgements

Appendix. Battery degradation mechanisms

Positive electrode and negative electrodes are collectively referred to as the "active material". The capacity of a battery to store electrical energy is determined by the amount of lithium ions that can be stored in these electrodes. When a battery is fully charged, lithium ions accumulate in the positive electrode, and as the battery discharges, they move from the positive electrode to the negative electrode. The charging process reverses the direction of the lithium ions. The state of health (SoH) of a battery depends on its ability to store and release lithium ions during the charging and discharging process. A battery's end-of-life is typically reached when it can no longer retain a sufficient fraction of its initial capacity. The battery capacity is determined by the amount of lithium that can be moved from one electrode to the other. This amount of lithium is commonly referred to as the "lithium inventory".

The most common ageing mode associated to battery degradation is the loss of lithium inventory (LLI), which is related to lithium consumption by parasitic reactions (e.g., electrolyte decomposition, solid electrolyte interface growth, etc.) [30]. The second ageing mode is the loss of active material (LAM), which commonly results from particle cracking and loss of electrical contact, among other causes [31]. The LAM can be further classified into four types, depending on the electrode (positive and negative) and the degree of lithiation (predominantly lithiated or delithiated state) [27]. These ageing modes (i.e., LLI and LAM) can lead to both to capacity and power fade.

Table A.4
Degradation mechanisms considered in this study and their influence in the latent variables.

Deterioration	Influence on latent variables
LLI	Capacities z_1, z_2, z_3 are maintained, initial electrode lithiation levels z_4, z_5 are altered
LAMdPE	Positive electrode capacity z_1 reduced, initial lithiation levels z_4, z_5 maintained
LAMdGr	Gr electrode capacity z_2 reduced, initial lithiation levels z_4, z_5 maintained
LAMdSi	Si electrode capacity z_3 reduced, initial lithiation levels z_4, z_5 maintained
LAMlPE	Positive electrode capacity z_1 is reduced, initial lithiation levels of the electrodes z_4, z_5 are altered
LAMlGr	Gr electrode capacity z_2 is reduced, initial lithiation levels z_4, z_5 of the electrodes are altered
LAMlSi	Si electrode capacity z_3 is reduced, initial lithiation levels z_4, z_5 of the electrodes are altered

In batteries with a negative electrode composed of a blended mix of graphite and silicon, such as those used in this study [28], we can distinguish six types of loss of active material: loss of capacity of the delithiated (LAMdPE) or lithiated (LAMlPE) positive electrode and loss of capacity in the graphite and silicon fractions of the negative electrode (LAMlGr, LAMdGr, LAMlSi, LAMdSi). In addition to the deteriorations related to the amount of energy that can be stored in a cell, there are other effects that limit the power that the cell can provide [27]. In the ohmic resistance increase the electrodes offer more resistance to the passage of current, which increases heat losses and reduces charging efficiency. In the faradaic rate degradation, the reaction rate between the electrode and the lithium ions is reduced, which prevents the energy from being extracted from the battery as quickly as necessary.

In summary, seven types of degradation mechanisms can be considered, shown in Table A.4 along with their relation with the values of the latent variables.

There are four types of degradation that influence only one of the latent variables:

$$\text{LLI}(\mathbf{z}(t), \alpha) = (z_1(t), z_2(t), z_3(t), z_4(t), z_5(t) + \alpha) \tag{44}$$

$$\text{LAMdPE}(\mathbf{z}(t), \alpha) = (z_1(t) - \alpha, z_2(t), z_3(t), z_4(t), z_5(t)) \tag{45}$$

$$\text{LAMdGr}(\mathbf{z}(t), \alpha) = (z_1(t), z_2(t) - \alpha, z_3(t), z_4(t), z_5(t)) \tag{46}$$

$$\text{LAMdSi}(\mathbf{z}(t), \alpha) = (z_1(t), z_2(t), z_3(t) - \alpha, z_4(t), z_5(t)) \tag{47}$$

and three additional types whose influence on the latent variables cannot be distinguished from a combination of two of the previous types (even though their electrochemical causes may be different)

$$\text{LAMlPE}(\mathbf{z}(t), \alpha) = \text{LLI}(\text{LAMdPE}(\mathbf{z}(t), \alpha), \alpha) \tag{48}$$

$$\text{LAMlGr}(\mathbf{z}(t), \alpha) = \text{LLI}(\text{LAMdGr}(\mathbf{z}(t), \alpha), \alpha) \tag{49}$$

$$\text{LAMlSi}(\mathbf{z}(t), \alpha) = \text{LLI}(\text{LAMdSi}(\mathbf{z}(t), \alpha), \alpha). \tag{50}$$

α is the severity of the deterioration, measured in charge units. Given two vectors of latent variables, determining the severities of the sequence of degradations that transforms one value into the other is an underdetermined numerical optimisation problem.

References

[1] Alaswad S, Xiang Y. A review on condition-based maintenance optimization models for stochastically deteriorating system. Reliab Eng Syst Saf 2017;157:54–63.

[2] Si X-S, Wang W, Hu C-H, Zhou D-H. Remaining useful life estimation–a review on the statistical data driven approaches. European J Oper Res 2011;213(1):1–14.

[3] Azar K, Hajiakhondi-Meybodi Z, Naderkhani F. Semi-supervised clustering-based method for fault diagnosis and prognosis: A case study. Reliab Eng Syst Saf 2022;222:108405.

[4] Nguyen V-T, Do P, Vosin A, Iung B. Artificial-intelligence-based maintenance decision-making and optimization for multi-state component systems. Reliab Eng Syst Saf 2022;228:108757.

[5] Wang Y, Li X, Chen J, Liu Y. A condition-based maintenance policy for multi-component systems subject to stochastic and economic dependencies. Reliab Eng Syst Saf 2022;219:108174.

[6] Liu X, Matias J, Jäschke J, Vatn J. Gibbs sampler for noisy transformed gamma process: Inference and remaining useful life estimation. Reliab Eng Syst Saf 2022;217:108084.

[7] Lee J, Mitici M. Multi-objective design of aircraft maintenance using gaussian process learning and adaptive sampling. Reliab Eng Syst Saf 2022;218:108123.

[8] Pang Z, Si X, Hu C, Du D, Pei H. A Bayesian inference for remaining useful life estimation by fusing accelerated degradation data and condition monitoring data. Reliab Eng Syst Saf 2021;208:107341.

[9] Prakash O, Samantaray AK. Prognosis of dynamical system components with varying degradation patterns using model–data–fusion. Reliab Eng Syst Saf 2021;213:107683.

[10] Zhang N, Cai K, Zhang J, Wang T. A condition-based maintenance policy considering failure dependence and imperfect inspection for a two-component system. Reliab Eng Syst Saf 2022;217:108069.

[11] Sánchez L, Costa N, Otero JJ, Couso I. Physics-informed learning under epistemic uncertainty with an application to system health modeling. Internat J Approx Reason 2023. Under Review.

[12] Guillaume R, Dubois D. A min–max regret approach to maximum likelihood inference under incomplete data. Internat J Approx Reason 2020;121:135–49.

[13] Lisbona D, Snee T. A review of hazards associated with primary lithium and lithium-ion batteries. Process Saf Environ Prot 2011;89(6):434–42.

[14] Rauf H, Khalid M, Arshad N. Machine learning in state of health and remaining useful life estimation: Theoretical and technological development in battery degradation modelling. Renew Sustain Energy Rev 2022;156:111903.

[15] Severson KA, Attia PM, Jin N, Perkins N, Jiang B, Yang Z, et al. Data-driven prediction of battery cycle life before capacity degradation. Nature Energy 2019;4(5):383–91.

[16] Sánchez L, Costa N, Anseán D, Couso I. Informed weak supervision for battery deterioration level labeling. In: Information processing and management of uncertainty in knowledge-based systems: 19th international conference, IPMU 2022, Milan, Italy, July (2022) 11–15, proceedings, Part II. Springer; 2022, p. 748–60.

[17] Hu C, Goebel K, Howey D, Peng Z, Wang D, Wang P, et al. Special issue on physics-informed machine learning enabling fault feature extraction and robust failure prognosis. Mech Syst Signal Process 2023;192:110219.

[18] Karniadakis GE, Kevrekidis IG, Lu L, Perdikaris P, Wang S, Yang L. Physics-informed machine learning. Nat Rev Phys 2021;3(6):422–40.

[19] Psaros AF, Meng X, Zou Z, Guo L, Karniadakis GE. Uncertainty quantification in scientific machine learning: Methods, metrics, and comparisons. J Comput Phys 2023;111902.

[20] Shinde K, Feissel P, Destercke S. Dealing with inconsistent measurements in inverse problems: Set-based approach. Int J Uncertain Quantif 2021;11(3).

[21] Latz A, Zausch J. Thermodynamic derivation of a Butler–Volmer model for intercalation in li-ion batteries. Electrochim Acta 2013;110:358–62.

[22] Winter M, Besenhard JO, Spahr ME, Novak P. Insertion electrode materials for rechargeable lithium batteries. Adv Mater 1998;10(10):725–63.

[23] Dubarry M, Baure G, Anseán D. Perspective on state-of-health determination in lithium-ion batteries. J Electrochem Energy Convers Storage 2020;17(4):044701.

[24] Shim J, Kostecki R, Richardson T, Song X, Striebel KA. Electrochemical analysis for cycle performance and capacity fading of a lithium-ion battery cycled at elevated temperature. J Power Sources 2002;112(1):222–30.

[25] Dubarry M, Svoboda V, Hwu R, Liaw BY. Incremental capacity analysis and close-to-equilibrium OCV measurements to quantify capacity fade in commercial rechargeable lithium batteries. Electrochem Solid-State Lett 2006;9(10):A454.

[26] Han X, Lu L, Zheng Y, Feng X, Li Z, Li J, et al. A review on the key issues of the lithium ion battery degradation among the whole life cycle. ETransportation 2019;1:100005.

[27] Dubarry M, Truchot C, Liaw BY. Synthesize battery degradation modes via a diagnostic and prognostic model. J Power Sources 2012;219:204–16.

[28] Anseán D, Baure G, González M, Cameán I, García A, Dubarry M. Mechanistic investigation of silicon-graphite/LiNi0.8Mn0.1Co0.1O2 commercial cells for non-intrusive diagnosis and prognosis. J Power Sources 2020;459:227882.

[29] Hüllermeier E, Destercke S, Couso I. Learning from imprecise data: Adjustments of optimistic and pessimistic variants. In: International conference on scalable uncertainty management. Springer; 2019, p. 266–79.

[30] Palacín MR. Understanding ageing in li-ion batteries: A chemical issue. Chem Soc Rev 2018;47(13):4924–33.

[31] Birkl CR, Roberts MR, McTurk E, Bruce PG, Howey DA. Degradation diagnostics for lithium ion cells. J Power Sources 2017;341:373–86.